

# miR-432 is a novel biomarker for PCNSL and is associated with cell adhesion: An integrated bioinformatics analysis

Qiang Ma (✉ [maqiang@xwhosp.org](mailto:maqiang@xwhosp.org))

---

Research

**Keywords:** miR-432, PCNSL, diagnosis, cell adhesion

**Posted Date:** March 10th, 2020

**DOI:** <https://doi.org/10.21203/rs.3.rs-16455/v1>

**License:**   This work is licensed under a Creative Commons Attribution 4.0 International License. [Read Full License](#)

---

## Abstract

**Background:** Primary central nervous system lymphoma (PCNSL), a rare form of the non-Hodgkin's lymphoma (NHL), usually has a poor prognosis, and molecular pathogenesis of PCNSL has not been fully elucidated. Here, potential miRNA biomarkers were investigated in patients with PCNSL using an integrated bioinformatics analysis.

**Methods:** Expression profile arrays (GSE122011, GSE139031, and GSE25297) were obtained from the Gene Expression Omnibus (GEO). Free-scale miRNA co-expression networks were constructed with 27 PCNSL patients from GSE122011 by the weighted gene co-expression network analysis (WGCNA) in order to identify candidate biomarkers. Subsequently, miRNA-miRNA networks were visualized with the Cytoscape. Expression of candidate miRNAs was assessed in serum samples from GSE139031, including 42 PCNSL patients and 77 non-cancer individuals, and the sensitivity and the specificity were assessed by the receiver operating characteristic (ROC) curve. From GSE25297, differentially expressed genes (DEGs) from the PCNSL tissues ( $n = 7$ ) and the normal lymph nodes ( $n = 7$ ) were compared, target genes of candidate miRNAs were downloaded from TargetScan database, and target genes that were also down-regulated in GSE25297 were used to construct the protein-protein interaction (PPI) networks and for the gene ontology (GO) analysis.

**Results:** miRNAs were clustered into two groups with 8 modules in 27 patients with PCNSL. One group consisted of the yellow and the turquoise modules, and the second group consisted of the other six modules. In the miRNA-miRNA network, the highest nodes were observed between miR-432 and miR-330-3p, which were from the yellow and the turquoise modules, and only miR-432 was closely associated with both the yellow ( $0.977$ ,  $P = 2.88E-18$ ) and the turquoise modules ( $0.525$ ,  $P = 0.005$ ). Additionally, patients with PCNSL had higher serum miR-432 expression compared with that in the non-cancer controls in GSE139031, and miR-432 has a higher accuracy for discriminating between PCNSL and non-cancer samples (AUC:  $0.77$ ; 95% CI:  $0.6923$  to  $0.8550$ ). For target genes of miR-432, RASGRF, DGKG, SMIM22, SPOCD1, NRCAM, CNTN2, PTPRD, POTED, IGSF3, SLC24A2, CTNND2, AIF1L, TMEM229A, GLDN, and MOBP were down-regulated in the PCNSL tissues. Among them, CTNND2, GLDN, NRCAM, and PTPRD were associated with cell adhesion.

**Conclusion:** Up-regulated miR-432 expression is a novel biomarker for patients with PCNSL and may be associated with cell adhesion.

## Background

Primary central nervous system lymphoma (PCNSL) is a rare subtype of the non-Hodgkin's lymphoma<sup>1</sup> and usually has a poor prognosis. Thus, accurate and timely diagnosis is necessary<sup>2</sup>. Until now, stereotactic biopsy has been the gold standard for PCNSL diagnosis<sup>3</sup>. Recently, discovery of molecular biomarkers from the cerebrospinal fluid (CSF)<sup>4</sup> and the serum<sup>5</sup> have become an area of extensive research. Among the novel biomarkers, microRNAs (miRNAs) have been considered in PCNSL diagnosis because the primary central nervous system diffuse large B-cell lymphoma (PCNS-DLBCL) has a distinct miRNA signature compared to that in the germinal center (GC)-DLBCL and the non-GC-DLBCL<sup>6</sup>. Despite this finding, there is a limited clinical application of miRNA. Hence, there is a necessity of further research into the discovery of diagnostic miRNAs using a variety of methods. In the present study, a combined analysis using multiple databases was performed, and key miRNAs associated with PCNSL were investigated with the goal of providing a theoretical basis for the development of diagnostic markers.

## Materials And Methods

Download and analysis of expression profiles from GEO.

Expression profiles of GSE122011, GSE139031, and GSE25297 were downloaded from the GEO database (<https://www.ncbi.nlm.nih.gov/gds>). MiRNA expression profiles from 27 patients with PCNSL were extracted from GSE12201. Serum miRNA expression profiles from 42 patients with PCNSL and 77 non-cancer controls were extracted from GSE139031. From GSE25297, differentially expressed genes in seven PCNSL and seven normal lymph node sets were screened using the R software ( $FDR < 0.01$  and  $\log_2$  fold change (FC, tumor-control)  $> 2$  or  $< -2$ ).

WGCNA and ROC analysis.

MiRNA co-expression networks from 27 patients with PCNSL from GSE12201 were constructed using WGCNA analysis with the WGCNA package in R. Modules of the highly correlated miRNAs, module membership (MM), and a module heatmap were created as per a previously reported method<sup>7</sup>. Sensitivity and specificity of each candidate miRNA in GSE139031 were evaluated by ROC analysis as per a previously reported method<sup>8</sup>.

PPI and GO analysis.

MiR-432 target genes were downloaded from the TargetScan ([http://www.targetscan.org/vert\\_72/](http://www.targetscan.org/vert_72/))<sup>9</sup>, and target genes shared with the down-regulated genes in GSE25297 were subjected to a protein-protein interaction analysis with the Search Tool for the Retrieval of Interacting Genes/Proteins (STRING) (<https://string-db.org/>)<sup>10</sup>. The GO analysis was performed for genes with the STRING interactions, including biological process (BP), molecular function (MF), and cellular component (CC).

Statistical methods.

IBM SPSS Statistics 21.0, GraphPad Prism version 5 and R software with corresponding packages were used to perform the statistical analysis. Relative miR-432 expression was compared with the independent t-tests, and  $P < 0.05$  was considered statistically significant.

## Results

Eight modules were constructed for miRNAs in PCNSL.

Co-expressed miRNAs in PCNSL were clustered into eight modules. Among them, the yellow and the turquoise modules constituted one subgroup, and the green, the black, the brown, the red, the blue, and the pink modules constituted another subgroup (Fig. 1A). Module clustering indicated that the yellow module had the highest correlation with the turquoise module (Fig. 1B). Additionally, higher miRNA expression overall was observed in the yellow and the turquoise modules (Fig. 1C).

miR-432 is closely associated with the yellow and the turquoise modules.

A miRNA-miRNA network was constructed for the top 20 miRNAs in the turquoise and the yellow modules to identify key miRNAs in PCNSL (Fig. 2A and Fig. 2B). A higher number of nodes was observed between miR-330-3p and miR-432 compared to those in other miRNAs in these two modules. Meanwhile, MM values of all miRNAs from these two modules were calculated, and only miR-432 was significantly associated with both modules (Table 1). These results suggested that miR-432 may be a key link between the yellow and the turquoise modules.

Table 1  
MM value of miRNAs from yellow and turquoise.

miRNA symbols	Module Color	MM turquoise	p.value MMturquoise	MM yellow	p.value MMyellow
hsa-miR-1180_st	turquoise	0.831533932	7.73424E-08	0.755493074	5.21944E-06
hsa-let-7e_st	turquoise	0.898647822	1.97129E-10	0.725194359	1.87477E-05
hsa-miR-181c-star_st	turquoise	0.701275949	4.60196E-05	0.674294639	0.000114912
hsa-miR-181d_st	turquoise	0.906062921	7.947E-11	0.673373502	0.000118364
hsa-miR-1301_st	turquoise	0.83909774	4.54851E-08	0.672131088	0.000123166
hsa-miR-125b_st	turquoise	0.857983461	1.06368E-08	0.666302517	0.000148065
hsa-miR-195_st	turquoise	0.767768656	2.94865E-06	0.642688908	0.000300314
hsa-miR-30a-star_st	turquoise	0.788139208	1.05519E-06	0.623979705	0.000505083
hsa-miR-497_st	turquoise	0.876727826	2.01544E-09	0.614743479	0.000645076
hsa-miR-99b_st	turquoise	0.949820568	3.98807E-14	0.613891849	0.000659542
hsa-miR-23b_st	turquoise	0.959223459	3.13691E-15	0.601286905	0.000909187
hsa-miR-99b-star_st	turquoise	0.883789448	1.00311E-09	0.596595108	0.001021139
hsa-miR-99a_st	turquoise	0.886858157	7.30358E-10	0.590983623	0.001170574
hsa-miR-30a_st	turquoise	0.866518967	5.14406E-09	0.590517276	0.001183804
hsa-miR-145_st	turquoise	0.616227391	0.00062053	0.584296649	0.001373067
hsa-miR-26a_st	turquoise	0.668821007	0.000136809	0.571434137	0.001848806
hsa-miR-324-3p_st	turquoise	0.682108684	8.90203E-05	0.541161641	0.003558269
hsa-miR-143_st	turquoise	0.551927072	0.00283888	0.526984653	0.004738315
hsa-miR-138-1-star_st	turquoise	0.685351317	7.98916E-05	0.526916151	0.004744737
hsa-miR-361-5p_st	turquoise	0.880178016	1.44107E-09	0.515253615	0.005951521
hsa-let-7b_st	turquoise	0.956827603	6.32129E-15	0.505320544	0.007174781
hsa-miR-125b-2-star_st	turquoise	0.966099589	3.23665E-16	0.501463927	0.007703607
hsa-miR-30c_st	turquoise	0.715206616	2.75744E-05	0.487804116	0.009847628
hsa-miR-128_st	yellow	0.531724602	0.004311482	0.978676951	1.05338E-18
hsa-miR-487b_st	yellow	0.556569317	0.002569442	0.978064376	1.49594E-18
hsa-miR-432_st	yellow	0.524728939	0.004953713	0.9768701	2.88352E-18
hsa-miR-127-3p_st	yellow	0.60785983	0.000770341	0.972053892	2.98886E-17
hsa-miR-138_st	yellow	0.544909925	0.00329193	0.970790774	5.1586E-17
hsa-miR-134_st	yellow	0.541974761	0.003498982	0.91302436	3.15475E-11
hsa-miR-409-3p_st	yellow	0.507996635	0.006826073	0.906233706	7.77564E-11
hsa-miR-149_st	yellow	0.753431143	5.7264E-06	0.863601855	6.62984E-09
hsa-miR-31_st	yellow	0.652996218	0.000222187	0.813879544	2.4279E-07
hsa-miR-383_st	yellow	0.57484895	0.001710419	0.792046667	8.5547E-07

miRNA symbols	Module Color	MM turquoise	p.value MMrquoise	MM yellow	p.value MMyellow
hsa-miR-769-5p_st	yellow	0.75825826	4.60278E-06	0.789553108	9.78532E-07
hsa-miR-125a-5p_st	yellow	0.819511057	1.70836E-07	0.783915088	1.31748E-06
hsa-miR-874_st	yellow	0.748878696	7.00504E-06	0.774319902	2.1433E-06
hsa-miR-138-2-star_st	yellow	0.508984239	0.006701044	0.591676986	0.00115114
hsa-miR-339-3p_st	yellow	0.601119059	0.000913	0.587562573	0.001270677

miR-432 can discriminate between PCNSL and non-cancer profiles robustly.

To identify whether abnormal miR-432 was also expressed in the peripheral circulation, serum miR-432 was determined in patients with PCNSL and non-cancer samples. The results confirmed that serum miR-432 was higher in patients with PCNSL compared with that in the non-cancer control (Fig. 3A;  $P < 0.0001$ ). The ROC curve for PCNSL generated with serum miR-432 has an AUC of 0.77 with a 95% confidence interval (CI) of 0.6923 to 0.8550 ( $P < 0.0001$ ), which suggests that miR-432 may be a potential discriminator between PCNSL and non-cancer profiles.

miR-432 may be involved in the regulation of cell adhesion in PCNSL.

To explore the potential biological function of miR-432 in PCNSL, down-regulated miR-432 target genes were screened. The miR-432 target gene set was downloaded from the TargetScan database, and genes down-regulated in PCNSL were analyzed in GSE25297 (Fig. 4A). Shared genes from these two databases were considered candidate target genes. They included RASGRF, DGKG, SMIM22, SPOCD1, NRCAM, CNTN2, PTPRD, POTED, IGSF3, SLC24A2, CTNND2, AIF1L, TMEM229A, GLDN, and MOBP (Fig. 4B). Among the genes, protein-protein interactions were found for GLDN, CNTN2, NRCAM, MOBP, PTPRD, CTNND2, and RASGRF1 (Fig. 4C). The GO analysis of these seven genes was performed using the "Analysis" function in STRING, and BP, MF, and CC and have been shown in Tables 2–4. Furthermore, we observed that four target genes, CTNND2, GLDN, NRCAM, and PTPRD were involved in regulating cell-cell adhesion.

Table 2  
Biological process of main target genes of miR-432.

No.	term description	FDR	matching proteins
1	neuronal ion channel clustering	7.39E-05	CNTN2,GLDN,NRCAM
2	neuron differentiation	0.00053	CNTN2,CTNND2,DGKG,GLDN,NRCAM,PTPRD,RASGRF1
3	neuron development	0.0013	CNTN2,CTNND2,DGKG,GLDN,NRCAM,RASGRF1
4	synapse organization	0.0013	CNTN2,CTNND2,NRCAM,PTPRD
5	clustering of voltage-gated sodium channels	0.0015	GLDN,NRCAM
6	presynaptic membrane organization	0.0023	CNTN2,PTPRD
7	nervous system development	0.0037	CNTN2,CTNND2,DGKG,GLDN,MOBP,NRCAM,PTPRD,RASGRF1
8	axonal fasciculation	0.0051	CNTN2,NRCAM
9	heterotypic cell-cell adhesion	0.0071	GLDN,NRCAM
10	regulation of synaptic plasticity	0.0071	CNTN2,RASGRF1,SLC24A2
11	cell-cell adhesion	0.0071	CTNND2,GLDN,NRCAM,PTPRD
12	cell adhesion	0.0078	CNTN2,CTNND2,GLDN,NRCAM,PTPRD
13	learning or memory	0.0144	CNTN2,RASGRF1,SLC24A2
14	regulation of neuronal synaptic plasticity	0.0144	CNTN2,RASGRF1
15	plasma membrane bounded cell projection organization	0.0144	CNTN2,CTNND2,GLDN,NRCAM,RASGRF1
16	regulation of cell morphogenesis involved in differentiation	0.0166	CNTN2,NRCAM,PTPRD
17	neuron projection development	0.0166	CNTN2,CTNND2,NRCAM,RASGRF1
18	system development	0.0183	CNTN2,CTNND2,DGKG,GLDN,IGSF3,MOBP,NRCAM,PTPRD,RASGRF1
19	synapse assembly	0.0236	NRCAM,PTPRD
20	membrane organization	0.0252	CNTN2,GLDN,NRCAM,PTPRD
21	memory	0.0409	RASGRF1,SLC24A2
22	cell morphogenesis involved in neuron differentiation	0.0409	CNTN2,CTNND2,NRCAM
23	neuron migration	0.0439	CNTN2,NRCAM
24	regulation of neuron projection development	0.0498	CNTN2,NRCAM,PTPRD
25	neuron projection morphogenesis	0.0498	CNTN2,CTNND2,NRCAM

Table 3  
Molecular function of main target genes of miR-432.

No.	term description	FDR	matching proteins
1	protein binding involved in heterotypic cell-cell adhesion	0.0036	GLDN,NRCAM

Table 4  
Cell component of main target genes of miR-432.

No.	term description	FDR	matching proteins
1	cell periphery	0.0203	AIF1L,CNTN2,DGKG,GLDN,IGSF3,MOBP,NRCAM,POTED,PTPRD,RASGRF1,SLC24A2
2	axon	0.0256	CNTN2,GLDN,NRCAM,RASGRF1
3	plasma membrane	0.0362	AIF1L,CNTN2,DGKG,GLDN,IGSF3,NRCAM,POTED,PTPRD,RASGRF1,SLC24A2
4	membrane	0.0362	AIF1L,CNTN2,DGKG,GLDN,IGSF3,NRCAM,POTED,PTPRD,RASGRF1,SLC24A2,SMIM22,TMEM229A
5	axon part	0.0362	CNTN2,NRCAM,RASGRF1
6	neuron projection	0.0362	CNTN2,CTNND2,GLDN,NRCAM,RASGRF1
7	main axon	0.0362	CNTN2,NRCAM
8	plasma membrane bounded cell projection	0.0362	AIF1L,CNTN2,CTNND2,GLDN,NRCAM,RASGRF1
9	plasma membrane bounded cell projection part	0.0362	AIF1L,CNTN2,CTNND2,NRCAM,RASGRF1
10	myelin sheath	0.043	CNTN2,MOBP

## Discussion

In this study, up-regulated miR-432 was found in the tumor tissues and in the serum of patients with PCNSL and was explored as a potential diagnostic biomarker for PCNSL. Compared with the normal lymph nodes, 15 miR-432 target genes were down-regulated in PCNSL and linked to a cell-cell adhesion. These results indicated that serum miR-432 may be a potential marker for identifying PCNSL, and miR-432 may be associated with the regulation of cell adhesion.

Although stereotactic biopsy is the gold standard for PCNSL diagnosis, non-invasive diagnostic methods are under investigation<sup>11</sup>, and liquid biopsy has been presented as a promising method<sup>2</sup>. MiR-30c in the CSF could serve as a biomarker to distinguish between PCNSL and SCNSL<sup>12</sup>. MiR-151a-5p and miR-151b exhibited the most prominent differences in the blood of patients with PCNSL<sup>13</sup>. Additionally, it is necessary to develop novel, more effective miRNA biomarkers because there are limited molecular biomarkers with a widespread clinical applicability. Recently, WGCNA was used for the development of disease-related diagnostic and prognostic markers by creating relationships between gene modules and clinic traits<sup>14</sup>. In this study, the WGCNA approach was used to construct the miRNA co-expression network from 27 patients with PCNSL. All miRNAs were divided into two groups with eight modules. The yellow and the turquoise modules consisted of a subgroup with a high correlation. In order to find the key miRNAs shared between these two modules, interaction networks of the top 20 miRNAs were constructed. In parallel, MM values of all miRNAs in these two modules were calculated. Finally, miRNA-432 was identified as a potential key miRNA due to the higher node number and close association between these two modules. In fact, an abnormal expression of miR-432 has been observed in multiple tumor tissues and linked to the drug resistance in tumors and the malignant phenotype. For example, miR-432-3p was highly expressed in the ESCC tumors compared with that in the corresponding non-cancerous esophageal mucosa, and up-regulated miR-432 could decrease sensitivity of the cancer cells to chemotherapeutic drugs<sup>15</sup>. MiR-432 has also been reported to play an important role in tumor progression; it can suppress tumor growth, but also promote tumor progression by regulating cell proliferation and

apoptosis<sup>16</sup>. In PCNSL, the expression and role of miR-432 remains unclear; our study is the first to demonstrate up-regulated miR-432 in patients with PCNSL.

MiRNAs, non-coding RNAs that can inhibit gene transcription, affect diverse biological processes by regulating expression of hundreds of target genes<sup>17</sup>. Here, in order to investigate the potential function of miR-432 in PCNSL, target genes of miR-432 that were down-regulated in PCNSL were selected, and the PPI and the GO analyses were performed. PPI were found among seven genes, and the genes were mainly involved in regulating cell-cell adhesion. A previous study found that ECM and adhesion-related pathways were implicated in PCNSL; adhesion molecules, such as MAG, contributed to cancer invasiveness<sup>18</sup>. Here, CTNND2, GLDN, NRCAM, and PTPRD, genes associated with cell-cell adhesion, were found to be the target genes of miR-432. This suggested that miR-432 may be involved in cell-cell adhesion by regulating target gene expression. However, some limitations of this study should be noted. First, verification should be performed on a larger sample of PCNSL profiles. Second, it is unclear whether up-regulated miR-432 may be implicated in other types of brain tumors and affect the diagnosis. Third, in vivo and in vitro experiments should be performed to validate the bioinformatics analysis in this study.

## Conclusions

In brief, serum miR-432 was up-regulated in patients with PCNSL and may be associated with the regulation of cell-cell adhesion. Thus, miR-432 may be a target for both diagnosis and treatment.

## Declarations

### Ethics approval and consent to participate

Not applicable.

### Consent for publication

Not applicable.

### Availability of data and material

All data generated during this study are included in this published article.

### Acknowledgements

Not applicable.

### Funding

Not applicable.

## Authors' contributions

QM made substantial contributions to the design of the study, data analysis and writing.

## Competing interests

The author declared that no competing interests.

## Author details

<sup>1</sup>Department of Hematology, Capital Medical University, Beijing 100053, P.R. China

Correspondence to: Dr Qiang Ma, Department of Hematology, Capital Medical University, No.45 Changchun Str. Beijing 100053, P.R. China.

Email: [maqiang@xwhosp.org](mailto:maqiang@xwhosp.org)

## References

1. Batchelor TT. Primary central nervous system lymphoma: A curable disease. *Hematol Oncol*. 2019;37(Suppl 1):15–8.
2. Hiemcke-Jiwa LS, Leguit RJ, Snijders TJ, et al. Molecular analysis in liquid biopsies for diagnostics of primary central nervous system lymphoma: Review of literature and future opportunities. *Crit Rev Oncol Hematol*. 2018;127:56–65.
3. Sinicrope K, Batchelor T. Primary Central Nervous System Lymphoma. *Neurologic clinics*. 2018;36:517–32.
4. Morell AA, Shah AH, Cavallo C, et al. Diagnosis of primary central nervous system lymphoma: a systematic review of the utility of CSF screening and the role of early brain biopsy. *Neuro-oncology practice*. 2019;6:415–23.
5. Ho KG, Grommes C. Molecular profiling of primary central nervous system lymphomas - predictive and prognostic value? *Curr Opin Neurol*. 2019;32:886–94.
6. Yang K, Wang S, Cheng Y, Tian Y, Hou J. Role of miRNA-21 in the diagnosis and prediction of treatment efficacy of primary central nervous system lymphoma. *Oncology letters*. 2019;17:3475–81.
7. Langfelder P, Horvath S. WGCNA: an R package for weighted correlation network analysis. *BMC Bioinform*. 2008;9:559.
8. Zweig MH, Campbell G. Receiver-operating characteristic (ROC) plots: a fundamental evaluation tool in clinical medicine. *Clinical chemistry*. 1993;39:561–77.
9. Agarwal V, Bell GW, Nam JW, Bartel DP. Predicting effective microRNA target sites in mammalian mRNAs. *eLife* 2015;4.
10. Szklarczyk D, Gable AL, Lyon D, et al. STRING v11: protein-protein association networks with increased coverage, supporting functional discovery in genome-wide experimental datasets. *Nucleic acids research*. 2019;47:D607-D13.

11.  
Rubenstein JL, Hsi ED, Johnson JL, et al. Intensive chemotherapy and immunotherapy in patients with newly diagnosed primary CNS lymphoma: CALGB 50202 (Alliance 50202). *Journal of clinical oncology: official journal of the American Society of Clinical Oncology*. 2013;31:3061–8.
12.  
Baraniskin A, Chomiak M, Ahle G, et al. MicroRNA-30c as a novel diagnostic biomarker for primary and secondary B-cell lymphoma of the CNS. *Journal of neuro-oncology*. 2018;137:463–8.
13.  
Roth P, Keller A, Hoheisel JD, et al. Differentially regulated miRNAs as prognostic biomarkers in the blood of primary CNS lymphoma patients. *European journal of cancer*. 2015;51:382–90.
14.  
Wan Q, Tang J, Han Y, Wang D. Co-expression modules construction by WGCNA and identify potential prognostic markers of uveal melanoma. *Exp Eye Res*. 2018;166:13–20.
15.  
Akdemir B, Nakajima Y, Inazawa J, Inoue J. miR-432 Induces NRF2 Stabilization by Directly Targeting KEAP1. *Molecular cancer research: MCR*. 2017;15:1570–8.
16.  
Zhang YP, Liu KL, Wang YX, et al. Down-regulated RBM5 inhibits bladder cancer cell apoptosis by initiating an miR-432-5p/beta-catenin feedback loop. *FASEB journal: official publication of the Federation of American Societies for Experimental Biology*. 2019;33:10973–85.
17.  
Esquela-Kerscher A, Slack FJ. Oncomirs - microRNAs with a role in cancer. *Nature reviews Cancer*. 2006;6:259–69.
18.  
Lim DH, Kim WS, Kim SJ, Yoo HY, Ko YH. Microarray Gene-expression Profiling Analysis Comparing PCNSL and Non-CNS Diffuse Large B-Cell Lymphoma. *Anticancer research*. 2015;35:3333–40.

## Figures

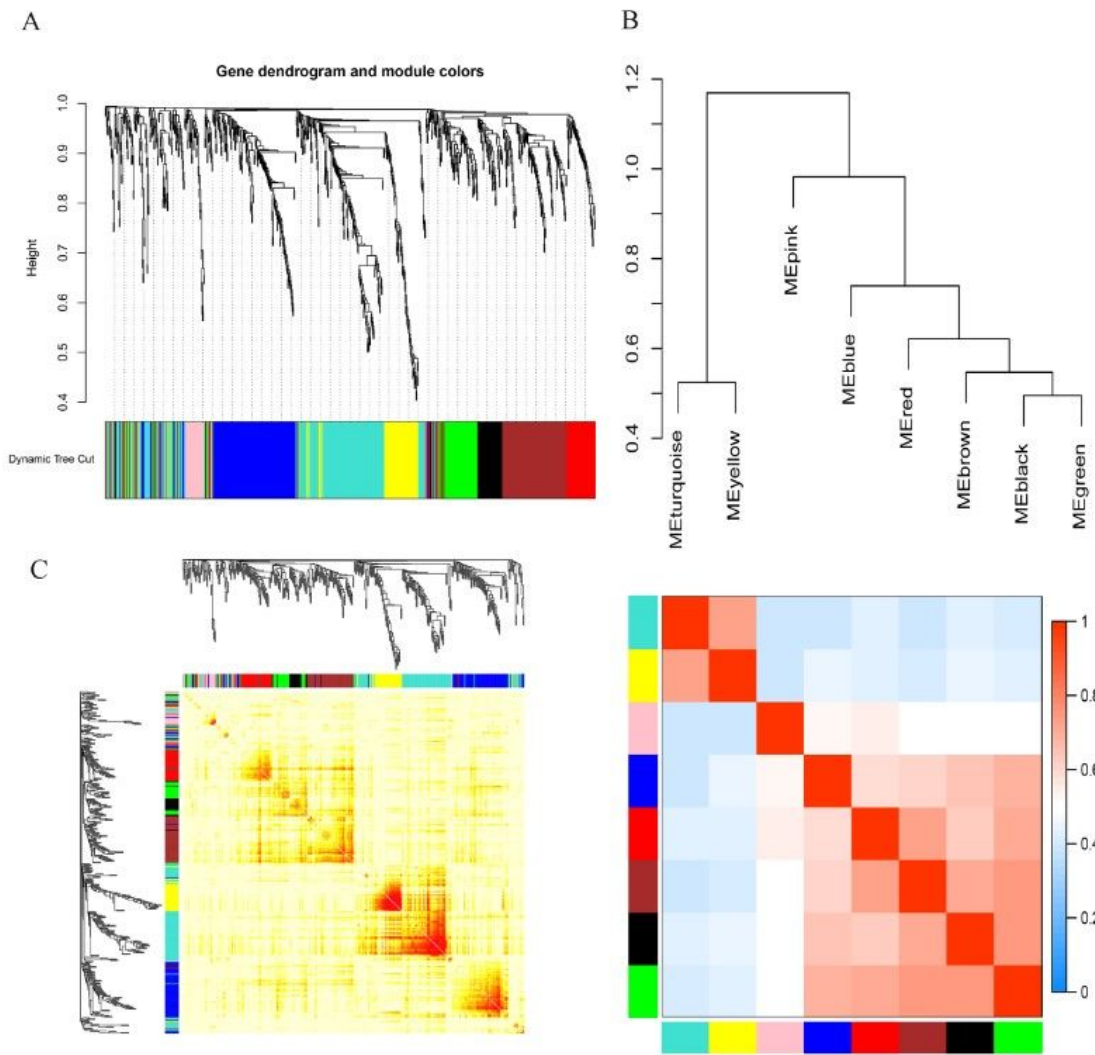


**Figure 1**

WGCNA analysis for miRNAs in GSE12201 (A) Gene dendrogram and module colors in the dynamic tree. (B) Heatmap of eight modules. (C) Heatmap for miRNAs in GSE12201.

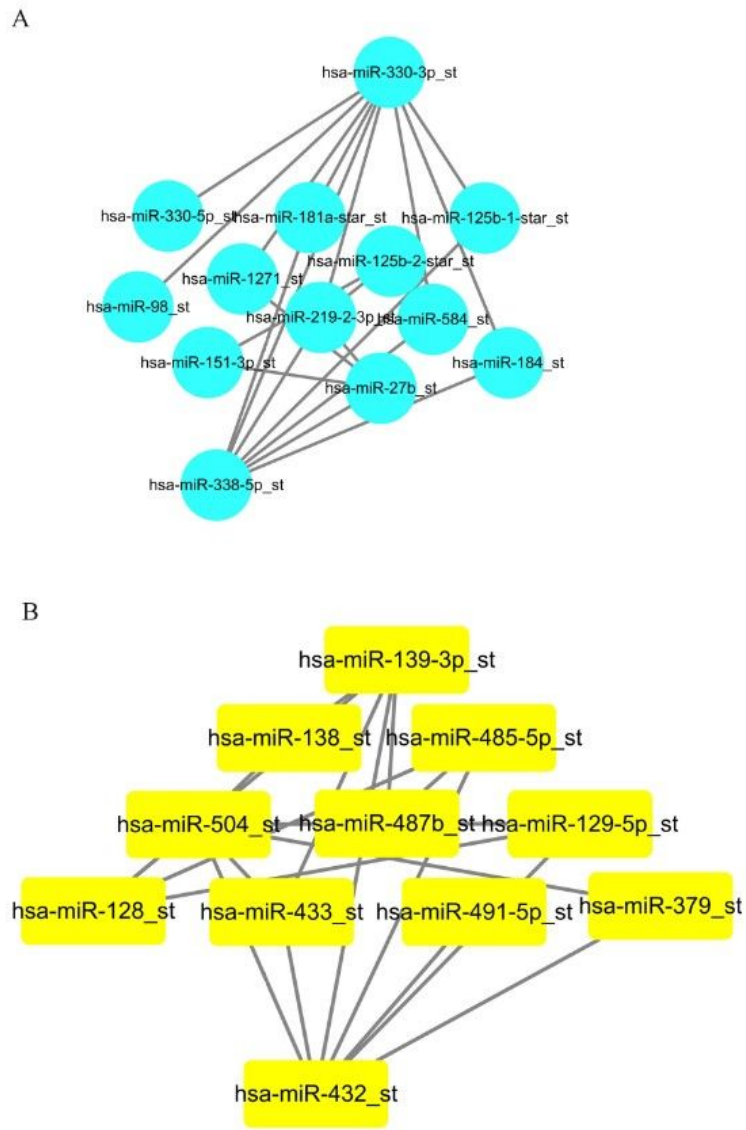


**Figure 4**

miRNA-miRNA co-expression network from turquoise and yellow modules (A) Co-expression network of top 20 miRNAs from the turquoise module. (B) Co-expression network of top 20 miRNAs from the yellow module.

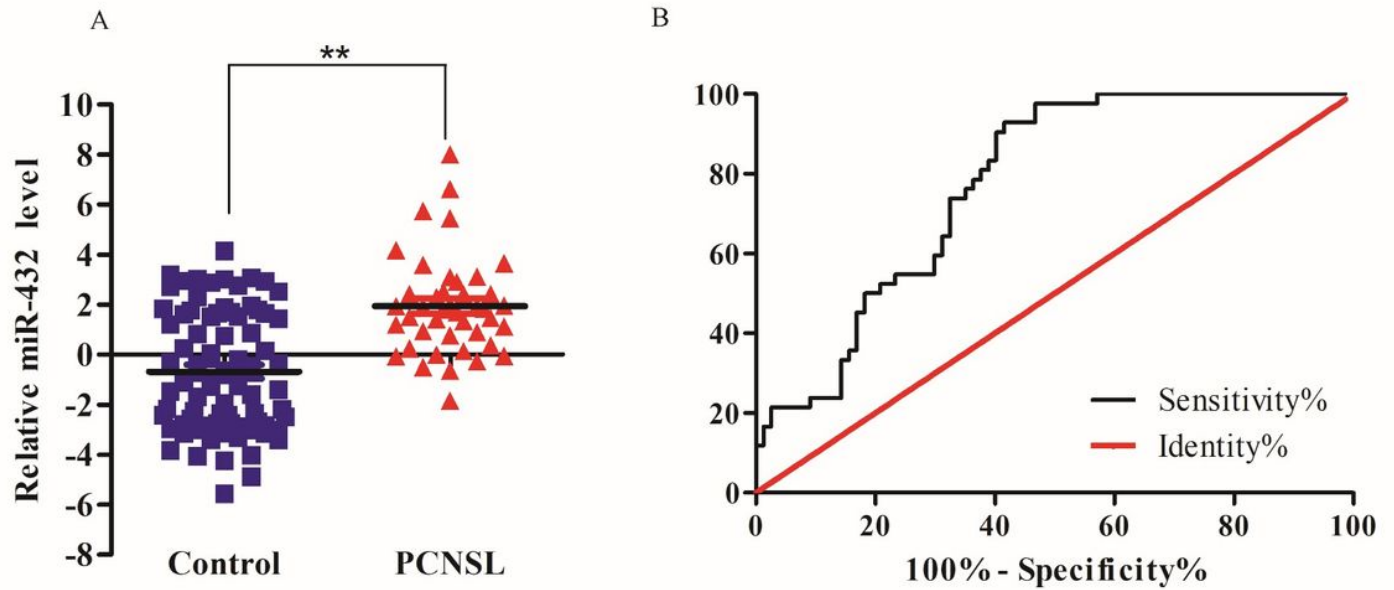


**Figure 6**

Up-regulated miR-432 is a robust determinant of PCNSL (A) Relative miR-432 expression was higher in serum of patients with PCNSL compared with that in the non-cancer control. \*\*: P < 0.0001. (B) ROC curve for serum miR-432 in patients with PCNSL.

